MICROSTRUCTURE-PROPERTY RELATIONSHIPS OF A ZINC OXIDE VARISTOR MATERIAL

Pamela Louise Williams
(M. S. thesis)

March 1979

Prepared for the U. S. Department of Energy
under Contract W-7405-ENG-48

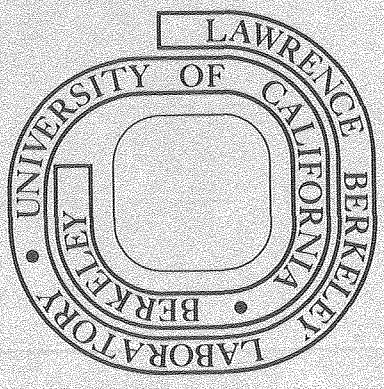

DISCLAIMER

MICROSTRUCTURE-PROPERTY RELATIONSHIPS OF A ZINC OXIDE VARISTOR MATERIAL

Pamela Louise Williams

ABSTRACT

Zinc oxide ceramics containing barium, cobalt, and rare earth metal oxides, which exhibit non-ohmic current-voltage characteristics, were studied. A new scanning electron microscopy technique has been developed to measure the voltage drop across grain boundaries. This was found to be ~2V. Detailed electron microscopic and spectroscopic observations showed that the barium and rare earth metals concentrate into small particles, embedded in the cobalt-doped zinc oxide grains. No intergranular films could be detected, to within 5Å resolution. Thus the nonlinear voltage characteristics are attributed to potential barriers arising from charge depletion layers formed adjacent to zinc oxide grain boundaries and two phase boundaries; experimental evidence is given to support this hypothesis.

MICROSTRUCTURE-PROPERTY RELATIONSHIPS OF A ZINC OXIDE VARISTOR MATERIAL

CONTENTS

Abstract

1. Introduction 1

    1.1. Varistor Usage 1

    1.2. Varistor Microstructure 1

    1.3. Varistor Electrical Characteristics 3

    1.4 Thesis Objectives 6

2. Experiments 6

    2.1. Bulk Sample Electrical Measurements 7

    2.2. Microstructure Analysis 8

    2.3. Voltage Contrast Experiment 9

3. Results and Calculations 10

    3.1. Bulk Sample Electrical Characteristics 10

    3.2. Microstructure Analysis 11

    3.3. Voltage Contrast Results 16

4. Discussion 18

5. Conclusions 21

Acknowledgements 22

References 23

Figures 25

1. INTRODUCTION

1.1. Varistor Usage

Electrical circuits and systems containing low cost, high reliability solid-state components are now being designed for use on power lines. These designs have to take into account that solid-state components cannot withstand some of the voltage surges imposed upon the circuits by power system transients. One type of transient protection device is the zinc oxide varistor, which is connected in parallel with the solid-state component to be protected. In normal operation, the varistor is an insulator with a resistivity of several mega ohm cms. It operates in the low-current prebreakdown region of the varistor's current-voltage characteristic where the current-voltage relationship is approximately linear. If a voltage surge impinges upon the solid-state load so that the total voltage applied to the load rises above the varistor's breakdown voltage, then the varistor current rapidly increases along its characteristic current-voltage curve, almost independent of voltage. The varistor becomes a conducting shunt path for the impinging voltage surge, thereby protecting the solid-state load.[1]

1.2. Varistor Microstructure

The zinc oxide varistor is a multi-component ceramic in which the electrical behavior depends on the ceramic microstructure and on the detailed processes occurring at zinc oxide grain boundaries. The primary constituent is zinc oxide, usually 95 mole percentage or more. In addition to the zinc oxide, the varistor contains smaller amounts of a number of other metal oxide constituents, such as: Al_2O_3, Bi_2O_3, CoO, Co_3O_4, Cr_2O_3,

MgO, MnO, NiO, Sb_2O_3, SiO_2, Sn_2O_3, TiO_2 and even rare earth metal oxides Pr_2O_3 and La_2O_3.[1,2]

The microstructure of previously studied zinc oxide varistors[1,3] consists of three phases: grains, particles, and intergranular material. The predominant phase is a matrix of randomly-oriented crystalline zinc oxide grains, which have substitutional doping of Co^{2+} ions for Zn^{2+} ions in the hexagonal zinc oxide crystal lattice. A secondary phase consists of aggregates of several metal oxides shaped into crystalline particles, that are frequently found at zinc oxide grain boundaries and occasionally within the grains. Thirdly, the intergranular material, also composed of several metal oxides, forms a three-dimensional threadlike network that wets the zinc oxide grains and partially isolates the grains from one another.[4]

Morris and Cahn[5] studied the simple zinc oxide--0.5 mole percent bismuth oxide varistor system. They observed an intergranular phase in the form of equilateral triangular prisms, located at three-grain junctions, leaving the center parts of the grain surfaces free of the intergranular phase; this phase was visible after one to three grains had been removed during fracture of the specimen. Using Auger electron spectroscopy on the fracture surface, they determined that the zinc oxide grain boundary was strongly enriched with bismuth, with the bismuth content decreasing rapidly over a distance of about 20 Å on either side of the grain boundary. They also observed a discontinuous thin film, much thinner than the network intergranular phase, on the grain surfaces. Clarke[6] studied grain boundaries in commercial (trade name GE-MOV) varistor samples using, for the first time, high-resolution transmission electron

microscopy techniques. He found an amorphous intergranular phase at all three and four grain junctions, amorphous thin films at boundaries parallel to the basal plane of a zinc oxide grain, but no continuous intergranular films or phases at other types of grain boundaries, thus confirming Morris and Cahn's observations.

1.3. Varistor Electrical Characteristics

By definition, varistors are voltage-dependent resistors, and zinc oxide varistors are semiconductor devices with non-linear current-voltage characteristics. The nonlinear electrical properties are usually described by the quantity α which is defined as $\alpha = (d\ln I)/(d\ln V) = VdI/IdV$, where I is the current through the varistor and V is the applied voltage. An ohmic material (like pure zinc oxide) has an α equal to one; and when α is infinity, the current varies infinitely for small changes in the applied voltage, and hence the varistor is perfect. Commercial varistors have maximum α values in the range of 30-50; these values depend on which metal oxides are added to the basic zinc oxide and the sintering temperature.[3]

In the prebreakdown region, the varistor current-voltage relationship exhibits a temperature dependence that can be described at constant voltage in terms of an activation energy. Bernasconi and his co-workers[7] measured the thermal activation energy and conductivity of GE-MOV varistors in this region as a function of zinc oxide concentration. They concluded that for zinc oxide concentrations larger than 96 mole percent, electrons are thermally excited over potential barriers at zinc oxide grain boundaries. Below 96 mole percent, the conductivity increases and the activation energy

decreases, the added metal oxides form the intergranular threadlike network, and conduction through this network increases with increasing concentration of metal oxides.

Levinson and Philipp[8] proposed that the conduction mechanism in the prebreakdown region is Schottky emission, where electrons are thermally excited over field-lowered potential barriers at the interfaces between zinc oxide grains and intergranular material. Emtage[9] envisioned the potential barriers as charge depletion layers about 1000 Å thick, at the edges of the zinc oxide grains. Electron traps in the intergranular layer absorb electrons from the zinc oxide grains so that depletion layers are formed in the zinc oxide. The conduction band of the depletion layers bend upward and rise above the intergranular conduction band, making the intergranular layer more conductive than the depletion layer.

Wong[10] found an average 2.3 volt drop (at 10^{-7} amperes, which is in the breakdown region) across the barrier between a zinc oxide grain and the intergranular phase, by correlating the GE-MOV varistor breakdown voltage with the mean zinc oxide grain size. This average, combined with the intergranular film thickness of 100 Å estimated from high-resolution transmission electron micrographs, leads to an electric field in the barrier greater than 10^6 volts/cm at the start of the breakdown region. Bernasconi et al.[7] used microcontact probes to measure the current-voltage characteristics of individual zinc oxide grain boundaries in the GE-MOV varistor. They found a two volt per boundary breakdown voltage, independent of zinc oxide concentration.

In the breakdown region, the current-voltage characteristic for the GE-MOV varistor is highly nonlinear with α greater than thirty for many

decades of current.[11] Levinson and Philipp[8] suggested that the conduction mechanism in this region is tunneling of electrons through field-narrowed potential barriers at the interfaces between zinc oxide grains and intergranular material. In contrast, in his charge depletion layer model, Emtage[9] hypothesized that when all the electron traps in the intergranular layer are filled, the barrier height decreases rapidly with a slight increase in voltage and then breakdown ensues. Breakdown occurs first in the regions where the intergranular layer is the thinnest.[9,11]

Mukae et al.[2] studied a zinc oxide based varistor material containing cobalt and rare earth metals, lanthanium and praseodymium. The microstructure consisted of zinc oxide grains uniformly doped with cobalt, surrounded by intergranular layers composed of La_2O_3-Pr_2O_3 solid solution. In the breakdown region, the value of α was about thirty, and the voltage drop across a grain boundary was 1.4 volts at 10^{-3} amperes, almost independent of composition.

For zinc oxide-rare earth metal oxide ceramics not doped with cobalt, only ohmic current-voltage characteristics were found, and in the pre-breakdown region, the resistivity was drastically increased by doping with cobalt. Mukae et al. concluded that the rare earth metal oxide layer has a low resistance and the nonohmic characteristics originate in the interface between the intergranular layer and the cobalt-doped zinc oxide grains, where charge depletion layers are formed. The rare earth metal oxides probably promote the sintering of the ceramic due to their high melting points and increase the density of energy states at the interface. Mukae et al. assumed that the rare earth metal oxides

behave as metals, so that the zinc oxide--intergranular layer--zinc oxide junction could be simulated as back to back Schottky diodes: when low voltage is applied, the electrons flow over potential barriers by Schottky emission; when high voltage is applied, the electrons tunnel through the potential barrier of the depletion layer from electron traps in the intergranular layer.

1.4. Thesis Objectives

The objective of this thesis was to find out whether the structures observed by Clarke[6] were typical of varistor materials by characterizing other ZnO based varistors using the highest levels of resolution currently available and then analyzing their microstructure-property relationships. The materials chosen for study were varistors supplied by TDK Electronics. Since the basic premise of the conduction theories relies on the presence of intergranular films, the importance of carrying out such a characterization is self-evident. At the same time a more direct study of the voltage characteristics was sought by utilizing a scanning electron microscope for voltage-current experiments.

The background information given above thus sets the stage for the following description of the experimental work and provides references with which the experimental results can be compared.

2. EXPERIMENTS

TDK Electronics, a Japanese industrial firm, provided three varistor samples for analysis. The samples have the same starting composition: 0.2 mole percent Nd_2O_3, 0.25 mole percent Sm_2O_3, 10 mole percent CoO, and presumably, 89.55 mole percent ZnO; but they differ in the way they

were manufactured (proprietary information) and in their current-voltage characteristics. The samples are black in color due to the metal oxide additives (usually pure zinc oxide ceramics are pale yellow) and came in the form of discs, ten to fourteen millimeters in diameter and about one millimeter thick. Taking this background information as a starting point, various experiments were performed on the samples to determine their microstructure so that this microstructure could be correlated with their electrical properties.

2.1. Bulk Sample Electrical Measurements

The bulk sample current-voltage characteristics supplied by the manufacturer were quite nonohmic, which indicates that the data represents part of the breakdown region. In order to determine where the breakdown region begins, an experiment was set up, according to the schematic of figure 1, to measure the low current-voltage relationships. The samples were prepared by lightly hand sanding and polishing the flat surfaces to remove surface contaminants; then a gold film contact about 500 Å thick was evaporated onto both these surfaces but not on the sides of the discs. For a measurement, a sample was placed in a test stand so that one surface made contact with a copper platform and the other surface made contact with a spring-restrained brass screw that held the sample in place on the platform. Then, a high voltage power supply (0-3000 volts DC, 0-10 milliamps) was connected to the test stand. The output from the specimen was connected to a Keithley Instruments Electrometer to measure the current, and the electrometer was grounded to the power supply. This electrometer was chosen because

it could measure a wide range of current values, from 10^{-10} to 10^{-2} amperes, and the scientific literature[1] indicated that the varistor electrical characteristics could vary over this wide range. The current-voltage relationships were obtained by incrementally increasing the power supply voltage and recording the corresponding current value found on the electrometer. The measurements were stopped at 200 volts so that the high current density would not overheat the specimen and change its microstructure.

2.2. Microstructure Analysis

Following the bulk specimen electrical measurements, the samples were again hand-sanded and polished to remove the gold film contacts and other surface contaminants, then etched in a dilute $HClO_4$ solution to slightly dissolve the zinc oxide grains so that grain boundaries and possible additional phases would be visible. Then, optical microscopy, scanning electron microscopy (SEM) and x-ray spectroscopy techniques, analyses, were used to investigate the microstructure and composition of the samples. For higher magnification studies, part of each sample was used to make the transmission electron microscopy (TEM) foils, as follows: the samples were sanded down to a thickness of ten mils, ultrasonically cut into two millimeter diameter discs, sanded and polished down to a thickness of about one mil, attached to 2.3 millimeter diameter copper grids with epoxy glue, then bombarded with argon ions in an ion milling machine until small holes appeared. At the edges of the holes, the specimens were thin enough for accelerated electrons to pass through. Then, a variety of transmission electron microscopy

techniques were employed: general bright field--dark field surveys; selected area electron diffraction; high-resolution weak-beam dark field and lattice fringe imaging in a Siemens 102 microscope; and x-ray compositional analyses using a 50 Å diameter probe in a Philipps 301 scanning-transmission electron microscope (STEM).

2.3. Voltage Contrast Experiment

In an attempt to more directly correlate the microstructure of specimens with their electrical properties, a new experiment was set up according to the schematic of figure 2. A bulk sample was hand sanded and polished, then lightly etched with dilute $HClO_4$ acid to reveal the zinc oxide grain boundaries. Next, a 0.1 millimeter diameter wire was taped across the sample so that it rested on the sample's surface. This wire was used as a mask when gold film contacts, about one micron thick, were evaporated onto the surface of the specimen. The resulting pattern was two gold film pads separated by a thin strip of zinc oxide varistor material. Then, the sample was attached with silver conducting paint to a piece of non-conducting glass, which in turn was attached to a specimen holder with two prongs. The prongs were carefully connected to the gold film pads with gold wire and silver paint. The specimen holder was installed in a scanning electron microscope and connected to cables leading out of the microscope to a power supply and a hundred ohm resistor. Voltmeters were connected across the power supply and the resistor to measure the applied voltage and the current through the circuit.

When electrons impinge on a specimen, secondary electrons are generated with a distribution of energies that can be detected and used to form an image in a scanning electron microscope. If the specimen potential voltage, initially at ground, is raised or lowered, then every emitted secondary electron loses or gains a proportional amount of energy; this change in energy causes a change in the image contrast, known as voltage contrast, which has been previously utilized for studying semiconductor devices.[12] So, scanning electron micrographs were taken of the zinc oxide strip as the applied voltage was varied, to detect this image change. If the video signal without the bias voltage is subtracted from the signal with the bias, the difference is proportional to the potential distribution in the specimen, at that particular bias voltage, and this distribution can be related to the specimen microstructure.

RESULTS AND CALCULATIONS

3.1. Bulk Sample Electrical Characteristics

Figure 3 shows the bulk specimen current-voltage characteristics for the three samples. In order to normalize the curves, the voltage data were divided by the sample thickness and the current data were divided by the contact area; thus, the slopes of the curves are proportional to the sample resistivity. Figure 4 shows the bulk specimen resistivity-voltage characteristics for the three samples. The slopes of the current-voltage curves, hence the resistivity, gradually decrease as the voltage increases throughout the selected voltage range; however, around 200 volts/mm, there is a change in the rate of decrease, indicating

the onset of breakdown. In the 80 to 200 volts/mm section of the curves, the current increases exponentially with voltage: $(I/A) = a_0 \exp(bV/t)$, where I is the varistor current, A is the contact area, V is the applied voltage, t is the sample thickness, and b is 0.034 to 0.036 mm/volt. Values of α, the nonlinear coefficient, range from one at 5 volts/mm to 28 or 29 at the upper reaches of the manufacturer's data.

Looking at the differences between the curves, above 20 volts/mm, sample 1 draws less current for a given applied voltage, and it has a higher breakdown voltage than the other two samples. From 40 to 200 volts/mm, the experimental data indicates that samples 2 and 3 have similar electrical characteristics, whereas the manufacturer's data indicates that they are quite different.

3.2 Microstructure Analysis

Figure 5 shows scanning electron micrographs of the three samples, taken at the same magnification. These micrographs show two phases: straight-sided zinc oxide grains and small particles, located at grain boundaries and within the grains. The main differences between the samples' microstructure are that sample 1 has the smallest mean zinc oxide grain size while sample 3 has the lowest population of particles. Elaborating on the first point, quantitative analysis of optical and scanning electron micrographs, following procedures outlined by Kingery et al.[13], revealed the mean zinc oxide grain width to be 9.8±1.3 microns, 11.7±1.9 microns, and 12.1±1.5 microns for samples 1, 2, and 3, respectively. For all three samples, the mean particle width is 1.5±0.7 microns, with larger but fewer particles at grain boundaries than within the grains.

Figure 6A shows high magnification scanning electron micrographs of sample 1. Except for the zinc oxide grain size, the microstructure revealed in these micrographs is typical of the microstructures of samples 2 and 3. Figure 6B shows the results of x-ray compositional analyses conducted in the scanning electron microscope on the phases marked A and B in figure 6A. The major limitation of this x-ray technique is its inability to detect the presence of oxygen or other elements with lower atomic numbers. According to the results, phase A contains zinc and cobalt, with a larger concentration of zinc than cobalt as indicated by the relative heights of their x-ray peaks; so, phase A is a zinc oxide grain doped with cobalt. In contrast, phase B contains zinc, cobalt, barium, neodymium, samarium, and possibly oxygen, with a larger concentration of zinc than the other elements except oxygen. These compositions are representative of the phases found in samples 2 and 3.

Initial surveys in the transmission electron microscope at fairly high magnification (125,000 times) showed the three samples' microstructure to be similar on a fine scale. Figure 7A is a transmission electron micrograph of sample 2. X-ray compositional analyses were conducted on points a through g; the locations of the points are only approximate. Overall, the results are comparable to the results of figure 6B. Using a procedure described by Goldstein et al.[14], the relative heights of the x-ray peaks were converted into atomic percentages; these percentages do not include oxygen because its presence could not be detected. Figure 7B shows plots of these percentages as a function of the distance from a zinc oxide grain boundary (point b)

and a two phase boundary (point f). In the middle of the grains, the zinc and cobalt contents are, respectively, 87.6±0.4 and 12.4±0.5 percent, and are 86.7±0.3 and 13.3±0.3 percent at zinc oxide grain boundaries. No barium, neodymium or samarium reside at the zinc oxide grain boundaries in concentrations greater than one atomic percent (the minimum detection level of this technique). In the zinc oxide grains near the particles, the zinc content drops from 88 to 69 percent, with the largest change occurring within 0.5 micron of the two phase boundary; the corresponding cobalt content changes very little. The particle composition varies from particle to particle: 47 to 54 percent zinc, 16 to 19 percent cobalt, 13 to 16 percent barium, 11 to 12 percent samarium, and 5 to 6 percent neodymium.

Analysis of selected area electron diffraction patterns of different orientations revealed the configuration of the unit cell for the two phases to be hexagonal. As an example, figure 8A shows the 100 orientation electron diffraction patterns for the zinc-cobalt oxide phase and the zinc-other metals oxide phase. From calibrated diffraction patterns, the unit cell height and width were determined to be, respectively, 5.20 Å and 3.25 Å, for the zinc-cobalt oxide phase; while for the zinc-other metals oxide phase, they are 9.99 Å and 6.22 Å with slight changes from particle to particle.

Evans[15], in his book, An Introduction to Crystal Chemistry, described the hexagonal lattice of zinc oxide as consisting of covalent bonding between the ions Zn^{2-} and O^{2+} in a tetrahedal arrangement; this is clinographically shown on the left side of figure 8B, with cobalt ions occasionally substituting for zinc ions. He gave estimated covalent

radii for this arrangement: 1.31 Å for Zn^{2-} and 0.66 Å for O^{2+}; this radius for Zn^{2-} is close to the 1.33 Å atomic radius of zinc. Since the x-ray compositional analysis disclosed that the zinc-other metals oxide phase contains a large percentage of zinc and cobalt, it was hypothesized that this phase has an arrangement of ions similar to the wurtzite form of zinc oxide. Then, using the atomic radii of the metals (1.25 Å for cobalt, 1.81 Å for neodymium and samarium, 2.17 Å for barium), the structure shown on the right side of figure 8B was formulated. This structure allows for variations in composition and for a slight change in the unit cell height, depending upon the locations of the neodymium, samarium, and barium ions.

The basic premise of the varistor conduction mechanism theories discussed in the introduction is that there is an intergranular phase or film between the zinc oxide grains. Thus far, scanning and transmission electron micrographs have not revealed the presence of such a phase in these samples, even at three and four grain junctions. So, two high-resolution transmission electron microscopy techniques were employed to study whether or not this phase existed: weak-beam dark field and lattice fringe imaging which can also indicate changes in lattice parameter over small regions ($\lesssim$20Å).[16]

Figure 9 shows low magnification bright field--dark field pairs of transmission electron micrographs of sample 2. The top pair shows a three-grain junction and the bottom pair shows a two phase boundary; all boundaries appear highly curved. Figure 10A shows a high magnification bright field--dark field pair of transmission electron micrographs of a typical three-grain junction. The fringes parallel to the grain boundaries

indicate that the boundaries are inclined with respect to the micrograph plane. The variation in width of the fringes demonstrate where the boundaries gradually curve. This curvature makes it difficult to view the boundaries edge-on so as to determine whether or not an intergranular film is present. At the junction itself there is not any substantial intergranular phase.

Figure 10B shows a high magnification bright field--weak beam dark field pair of micrographs of a zinc-cobalt oxide grain boundary; in fact, they are enlargements of figure 10A. The narrow strip about 10 Å wide at the boundary could indicate a slight inclination of the boundary or suggest the presence of an intergranular film. One technique[17] used to clearly image thin intergranular films is to form a dark field image from electrons diffracted just from the film. In this case, the resulting micrograph consists of a bright thin streak, representing the film, against a dark background, which would be the grains bordering the film. However, after careful work, this technique did not reveal any films in these samples. Figure 10C shows a high magnification bright field--weak beam dark field pair of micrographs of a two phase boundary, with the zinc-cobalt oxide grain on the right side of each picture. The boundary appears fairly abrupt and highly curved.

Figure 11 shows a lattice fringe image transmission electron micrograph of a zinc-cobalt oxide grain boundary. Analysis of electron diffraction patterns indicated that for the grain on the right, the main diffracting atomic planes are 011 type, whose interplanar spacing is 2.5 Å. For the other grain, the main diffracting atomic planes are

$2\bar{1}0$ type, whose interplanar spacing is 1.6 Å. At the grain boundary, the lattice fringes from the two grains overlap, indicating that the boundary is slightly inclined relative to the micrograph plane. The boundary consists of a series of 2.5 Å high ledges made of atom rows. The width of the boundary is about 5 Å, and no intergranular film can be resolved. Since the 011 planes contain only one type of ion, either zinc or oxygen, a change in composition from zinc to cobalt ions theoretically should result in a change in the interplanar spacing. So, the width of the fringes in the right-hand grain were measured as a function of distance from the boundary to see if any change could be detected. Within the resolution of the micrograph, there does not appear to be any change in the fringe width. Thus, the change in composition, if there is one, could not be detected by this technique.[16]

3.3. Voltage Contrast Results

Figure 12 shows three scanning electron micrographs from the voltage contrast experiments. The strip in the middle of each picture is the zinc oxide varistor material, and on either side of it are the gold film contacts. For the micrograph on the left, no bias was applied across the contacts, and the contrast is due to the topography of the specimen. For the micrograph on the right a ten volt bias was applied across the contacts, so that superimposed on the topographical contrast, there is a voltage induced contrast which causes a dramatic contrast change to occur at grain boundaries. For the middle micrograph, the polarity of the bias was reversed and the consequent contrast reverses from that of the right-hand micrograph. In addition, the center micrograph

shows a series of potential steps across the varistor strip, with changes in potential again occurring at grain boundaries. To ensure that this observed phenomenon was not a product of etching the grain boundaries, the experiment was repeated on an unetched specimen, and similar results ensued.

Figure 13A shows scans of the video signal along a horizontal line across the varistor strip. Unfortunately, with the particular microscope used, it is not possible to know which horizontal line of the varistor image is being scanned. Figure 13B shows labeled traces of the line scans of figure 13A, accompanied by the calibrated difference between the applied bias and no bias scans. These differences show how the potential voltage varies across the varistor strip. The difference between the no bias scan and the 20-volt bias scan indicates that the potential uniformly increases from left to right across the strip, while the difference between the no bias scan and the 20-volt-reverse bias scan indicates that the potential decreases from left to right, with some possible sharp drops. The exact magnitude of these drops, if they exist, cannot be determined because the video signals are so noisy.

In order to decrease the noise factor, microdensitometer traces of the negatives of the voltage contrast micrographs were taken along a line marked A-A' in figure 12; these traces are displayed in figure 14. Figure 14A shows the no bias, 5-volt bias, and 5-volt-reverse bias traces accompanied by the difference between the no bias trace and the 5-volt bias trace and the difference between the no bias trace and the 5-volt-reverse bias trace. The latter difference curve discloses a 3.9

volt potential rise taking place over a ten micron wide region in the varistor, which is the mean grain size. Upon reversing the bias polarity, this region experiences a potential drop that could be as large as 3.2 volts; the static of the traces makes it difficult to tell the exact magnitude. Figure 14B shows the no bias, 10-volt bias, and 10-volt-reverse bias traces along with the two difference curves. One difference curve discloses a 5.9 volt potential rise over the same region found in figure 14A, and upon reversing the bias, this region has a 3.9 volt potential drop. Figure 14C shows the no bias, 20-volt bias, and 20-volt-reverse bias traces as well as the two difference curves. In this figure, the region in question experiences a 3.2 volt rise, then a 3.7 volt drop upon reversing the bias. At this bias, the current started to rapidly increase, indicating the onset of breakdown. Comparing the results of the different biases, as the applied bias increases, the potential is more evenly distributed across more grains in the varistor strip. The average voltage drop across a grain boundary is $\sim$2V.

4. DISCUSSION

Summarizing some of the experimental findings, the three varistor samples have a microstructure consisting of two phases: zinc oxide grains uniformly doped with cobalt (evidenced by the minimal change in composition throughout the zinc oxide grain, as shown in figure 7B), and small particles composed of a zinc-other metals oxide solution (evidenced by the variation in composition and lattice parameters from particle to particle). The other metals are cobalt, barium, samarium, and neodymium, in order of decreasing

concentration. Due to the high melting points of the rare earth metal oxides, the particle phase probably promotes the sintering of the ceramic, as suggested by Mukae et al.[2] No intergranular films could be detected.

The three varistor samples differ in their bulk specimen electrical characteristics, their mean zinc oxide grain size and their particle population. The sample with the smallest mean grain size and the largest particle population has the highest resistivity and breakdown voltage. Small grains have more surface area per unit volume than large grains; and if the surface area (grain boundary area) acts as a barrier to conduction, as proposed by several researchers[2,8,9], then a small-grained material would have a higher resistivity than a large-grained material. Likewise, a large particle population provides a large two phase boundary area, which conceivably could act as a barrier to conduction and thereby increase the resistivity.

The maximum α values of 28 or 29 for these samples are comparable to those for the commercial GE-MOV varistor.[3] Correlating the samples' breakdown voltage with their mean zinc oxide grain size gives a 2.0 volt drop per grain boundary at the start of breakdown. The exponential relationship between current and voltage for the 80 to 200 volts/mm section of figure 3 coincides with Emtage's charge depletion layer model.[9] He proposed that the current density (I/A) is an exponential function of the potential barrier height, which in turn is directly proportional to the bias voltage, for prebreakdown voltages. He noted that the rate of increase of current with voltage need not be very rapid, which accounts for the small b values found for the $(I/A) = a_0 \exp(bV/t)$ expression. The manufacturer supplied

current-voltage characteristics for samples with different starting compositions. The sample with the lowest cobalt concentration had the lowest resistivity and breakdown voltage, which tallies with the results of Mukae et al.

Inasmuch as no intergranular phase or film could be detected in these samples, even by high-resolution transmission electron microscopy, what could take the place of this phase in the conduction mechanisms discussed in the introduction? The answer is the zinc oxide grain boundaries themselves, via a space charge layer model[7], and/or the second phase particles.

If the rare earth metals provide electron traps, as assumed by Mukae et al., then charge depletion layers could exist in the zinc oxide grains adjacent to the particles. The overall voltage contrast results support the case for the grain boundaries. Unfortunately, the resolution of the voltage contrast micrographs is not fine enough to clearly delineate the image contrast near individual particles, due to the noisy video signal. However, on the scanning electron microscope screen, a definite reversal of contrast from light to dark was observed in the zinc oxide grains near large particles, upon reversing the bias voltage polarity; during this reversal, the zinc oxide grain on the opposite side of a particle would change from dark to light. The affected areas in the grains were about a micron in width, and the regions immediately surrounding these areas did not change in contrast upon changing the bias. This phenomenon indicates that potential drops occur locally near particles, which supports the charge depletion layer hypothesis.

Further study at higher magnification and better resolution is needed to explore the charge depletion layer hypothesis in more detail. One technique that might be employed is the electron beam induced current technique.[18] In this technique, the electron beam of the scanning electron microscope is used to locally induce a specimen to generate charge carriers, which may move in response to an internal electric field and produce a measurable "electron beam induced" current in an external circuit; the resolution of this technique is about 0.5 microns laterally. In addition, measurements of AC properties as a function of frequency would aid in comparing experimental observations with theoretical models.

5. CONCLUSIONS

The varistor samples from TDK Electronics have good nonohmic properties with α values of 29 or more. They have a microstructure consisting of two phases: zinc oxide grains uniformly doped with cobalt, and small particles composed of a zinc-other metals oxide solid solution. The other metals are cobalt, barium, samarium, and neodymium, in order of decreasing concentration. The particles are one to two microns in width and are located at grain boundaries and within the grains, with larger but fewer particles at grain boundaries. No intergranular films could be resolved. Due to the high melting points of the rare earth metal oxides, the particle phase probably promotes the sintering of the ceramic. Samples with small mean grain size and large particle populations have high resistivity and breakdown voltages; this indicates that the grain boundary area and the two phase boundary area act as barriers to conduction

and thereby increase the resistivity. Voltage contrast experimental results and bulk specimen electrical characteristics indicate that the conduction mechanism in these varistors can be explained by a charge depletion layer model.

ACKNOWLEDGEMENTS

The author wishes to express gratitude to Professor Gareth Thomas for his encouragement and guidance during the conduction of this research, and to M. Yodogawa of the TDK Electronics Company for providing the varistor samples and background information. Appreciation is extended to Dr. O. L. Krivanek, Dr. T. E. Everhart and Y. C. Lin for their contributions to the voltage contrast work. Appreciation is also extended to Dr. R. Gronsky, Dr. R. Mishra, Dr. U. Dahmen, T. Shaw, T. Roth, C. Gosnell, and M. F. Sung for their contributions to the transmission electron microscopy work. The assistance of Dr. R. Geiss in the compositional analysis conducted on the Philipps 301 microscope is also acknowledged. The U.S. Department of Energy through the Materials and Molecular Research Division of the Lawrence Berkeley Laboratory provided research facilities, technical staff, and financial support.

REFERENCES

1. Lionel M. Levinson and H.R. Philipp, G.E. Report 11 CRD110 (May 1977).

2. Kazuo Mukae, Koruchi Tsuda and Ikuo Nagasawa, Japan. J. Appl Phys., 16, 1361-1368 (1977).

3. Michio Matsuoka, Japan. J. Appl. Phys., 10, 736-746 (1971).

4. Joe Wong, J. Appl. Phys., 46, 1653-1659 (1975).

5. W.G. Morris and J.W. Cahn, Grain Boundaries in Engineering Materials (Baton Rouge, Louisiana: Claitors, 1975). William G. Morris, J. Vac. Sci. Tech., 13, 926-931 (1976).

6. David R. Clarke, J. Appl. Phys., 49, 2407-2411 (1978).

7. J. Bernasconi, H.P. Klein, B. Knecht and S. Strassler, J. Electronic Materials, 5, 473-495 (1976).

8. Lionel M. Levinson and H.R. Philipp, J. Appl. Phys., 46, 1332-1341 (1975).

9. P.R. Emtage, J. Appl. Phys., 48, 4372-4384 (1977).

10. Joe Wong, J. Appl. Phys., 47, 4971-4974 (1976).

11. H.R. Philipp and Lionel M. Levinson, J. Appl. Phys., 48, 1621-1627 (1977).

12. A. Gopinath, K.G. Gopinathan and P.R. Thomas, Scanning Electron Microscopy/1978, Vol. I (AMF O'Hare, Illinois: SEM Inc., 1978), pp. 375-380.

13. W.D. Kingery, H.K. Bowen and D.R. Uhlman, Introduction to Ceramics (New York: John Wiley & Sons, 1976), pp. 523-530.

14. J.I. Goldstein, J.L. Costley, G.W. Lorimer and S.J.B. Reed, Scanning Electron Microscopy/1977, Vol. I, Proceedings of the Workshop on Analytical Electron Microscopy (Chicago, Illinois: III Research Institute, March 1977), pp. 315-323.

15. R.C. Evans, An Introduction to Crystal Chemistry, Second Edition (Cambridge, England: Cambridge University Press, 1976), pp. 62-63, 70-74, 87, 133-135.

16. R. Sinclair, R. Gronsky and G. Thomas, Acta Met 24, 789 (1976).

17. O. L. Krivanek, T.M. Shaw and G. Thomas, in Press, J. Appl. Phys., LBL Report 7696 (Dec. 1978).

18. H.J. Leamy, L.C. Kimerling and S.D. Ferris, Scanning Electron Microscopy/1978, Vol. I (AMF O'Hare, Illinois: SEM Inc., 1978), pp. 717-724.

FIGURE 1:
BULK SAMPLE CURRENT-VOLTAGE MEASUREMENT EXPERIMENT SCHEMATIC

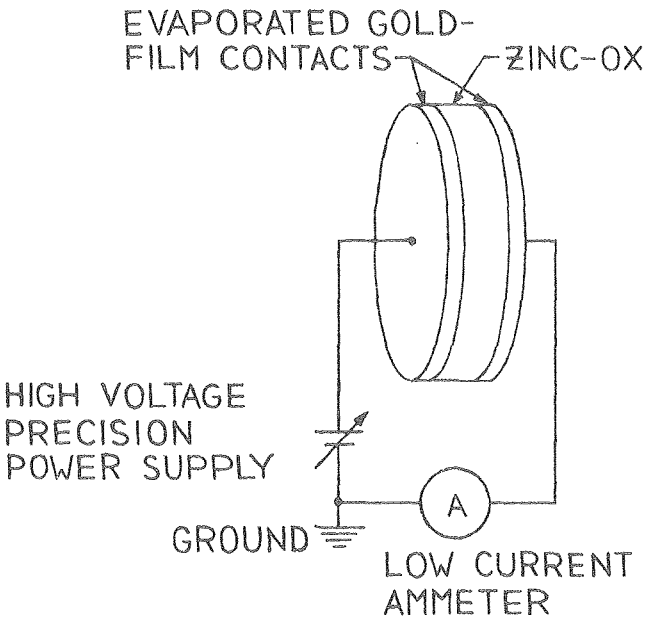

XBL 791-8031

Fig. 1

FIGURE 2:
VOLTAGE CONTRAST EXPERIMENT SCHEMATIC

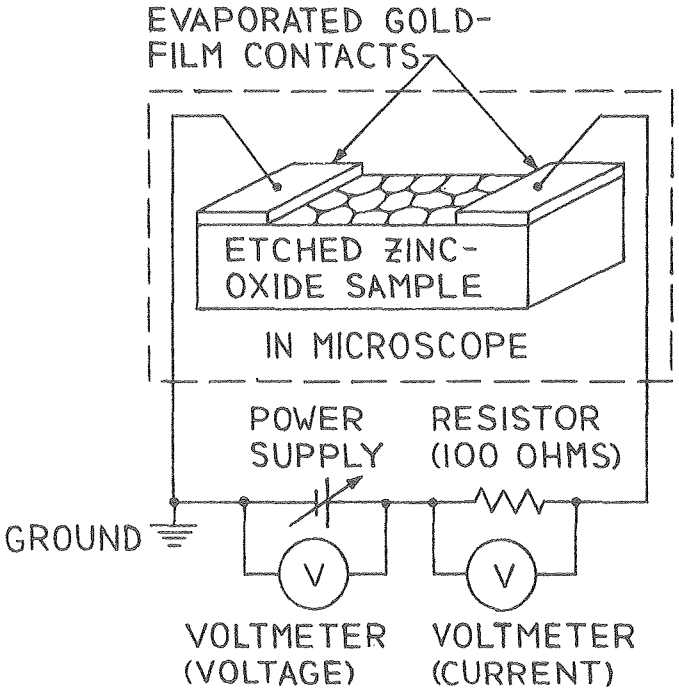

XBL 791-8033

Fig. 2

FIGURE 3: BULK SAMPLE CURRENT-VOLTAGE CHARACTERISTICS

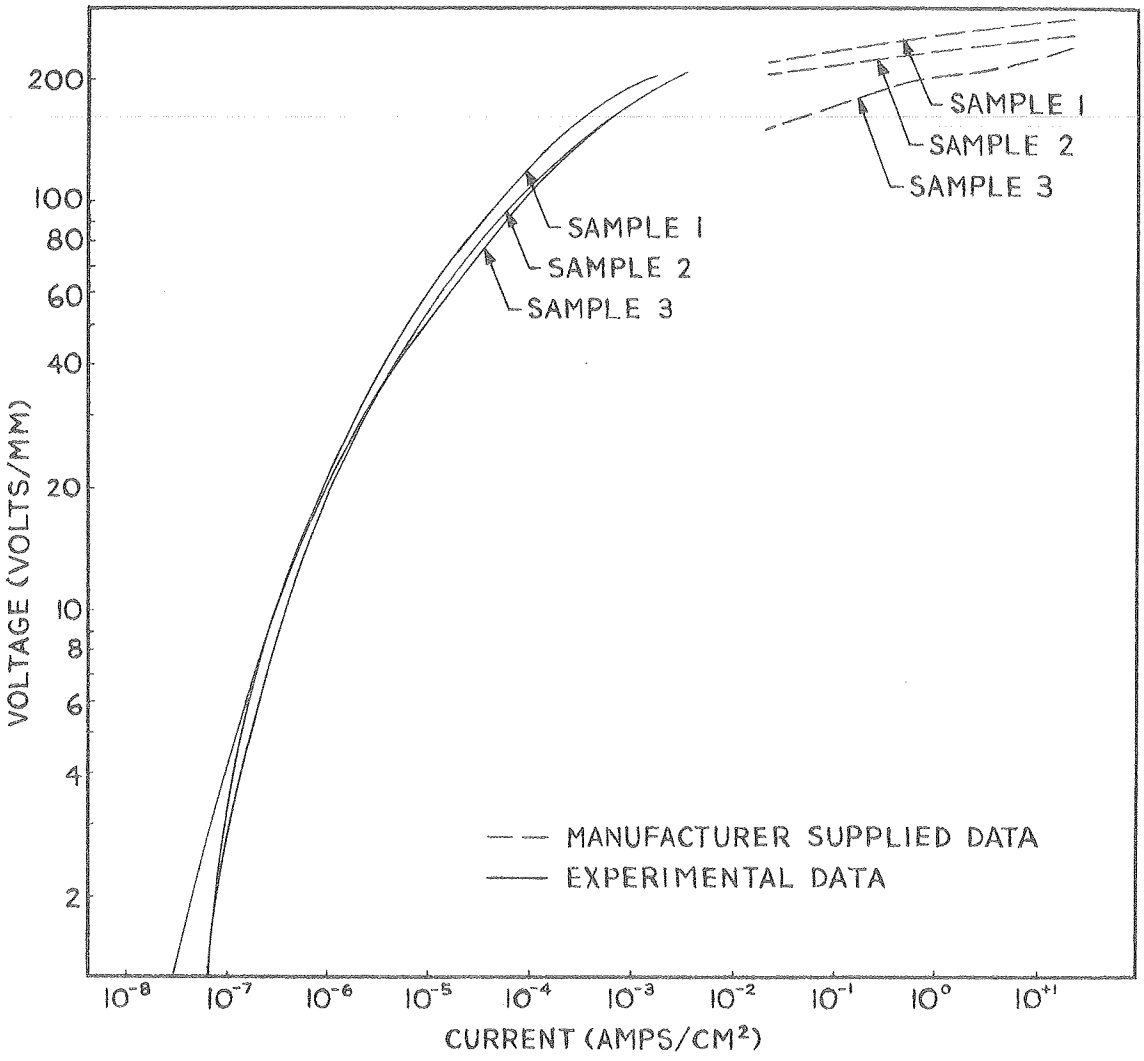

XBL 791-8028

Fig. 3

FIGURE 4
BULK SAMPLE RESISTIVITY-VOLTAGE CHARACTERISTICS

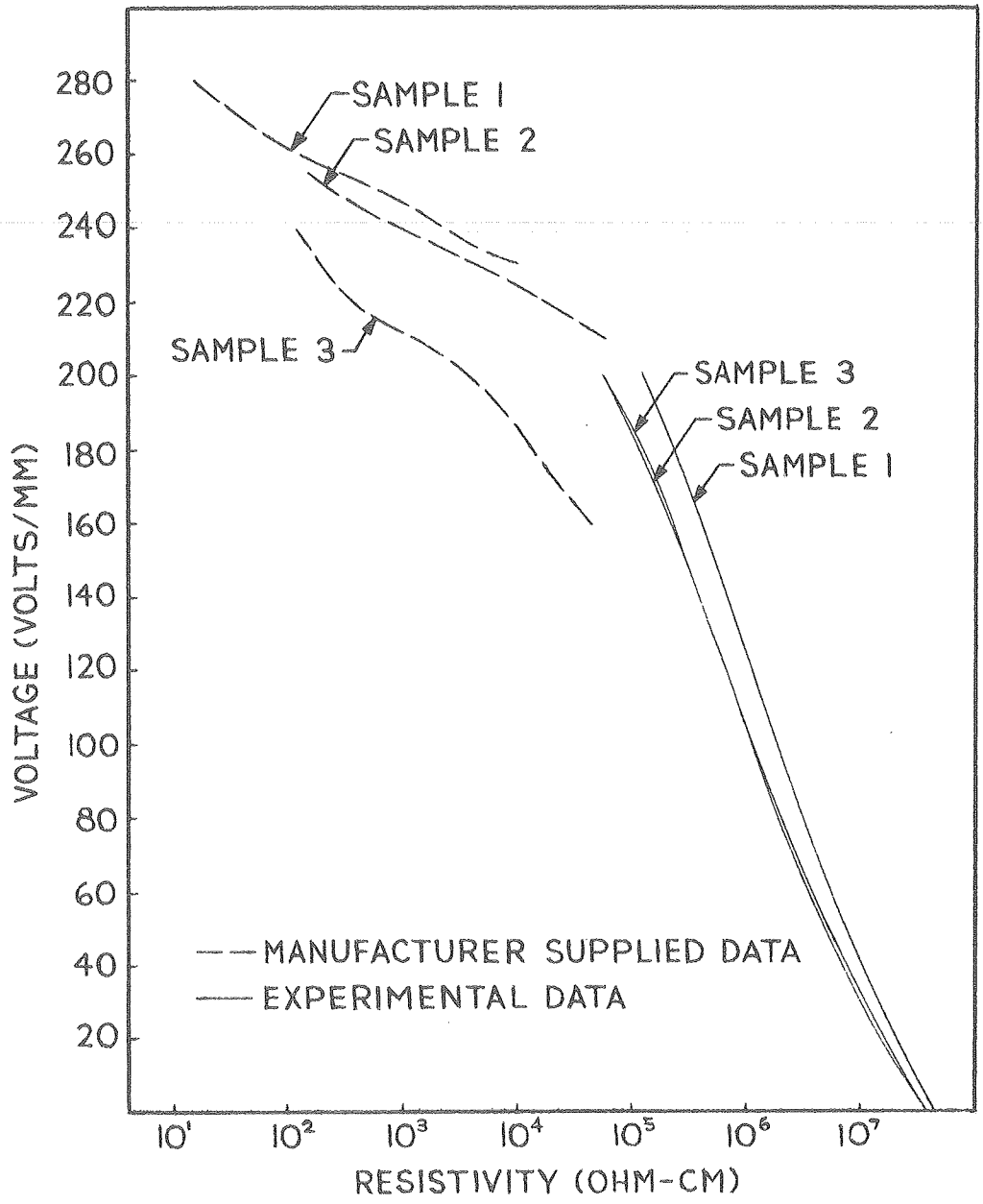

XBL 791-8034

Fig. 4

Figure 5
SEM MICROGRAPHS

SAMPLE 1

SAMPLE 2

SAMPLE 3

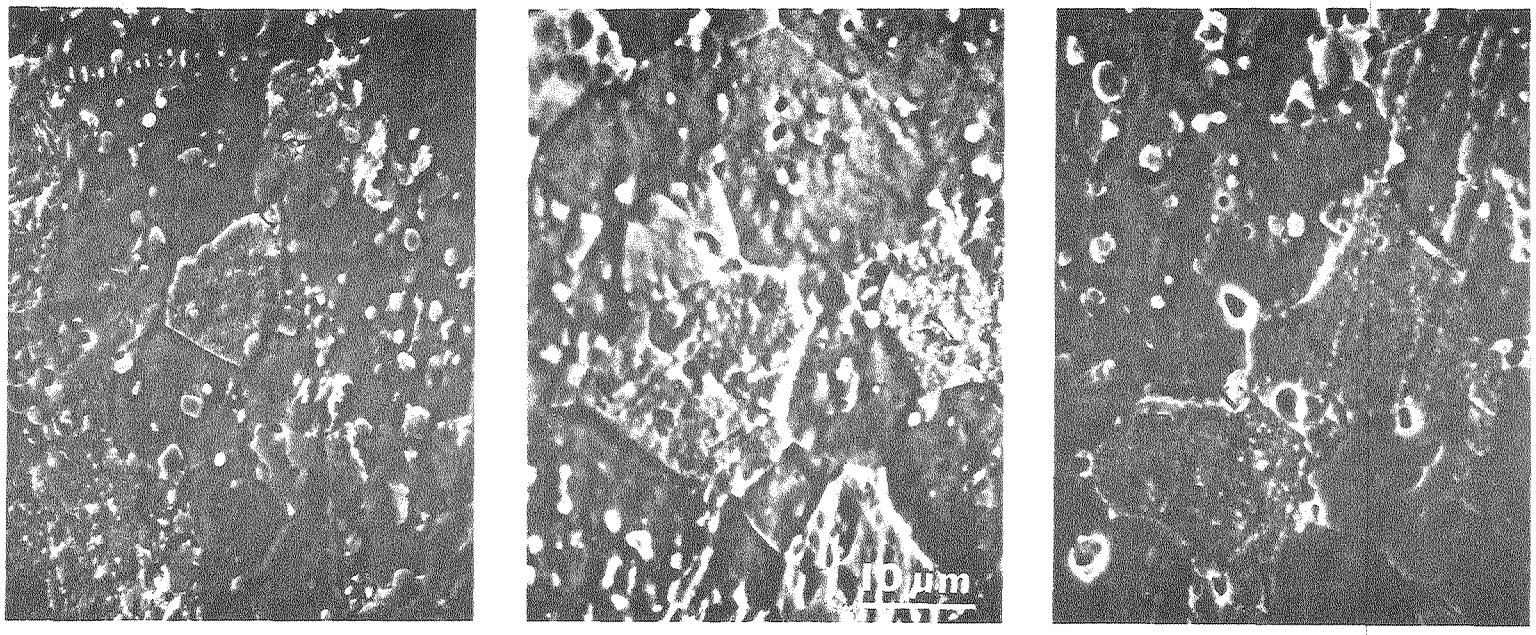

XBB 791-552

Fig. 5

Figure 6a

HIGH MAGNIFICATION SEM MICROGRAPHS
PHASE A: ZINC-COBALT OXIDE
PHASE B: ZINC-OTHER METALS OXIDE

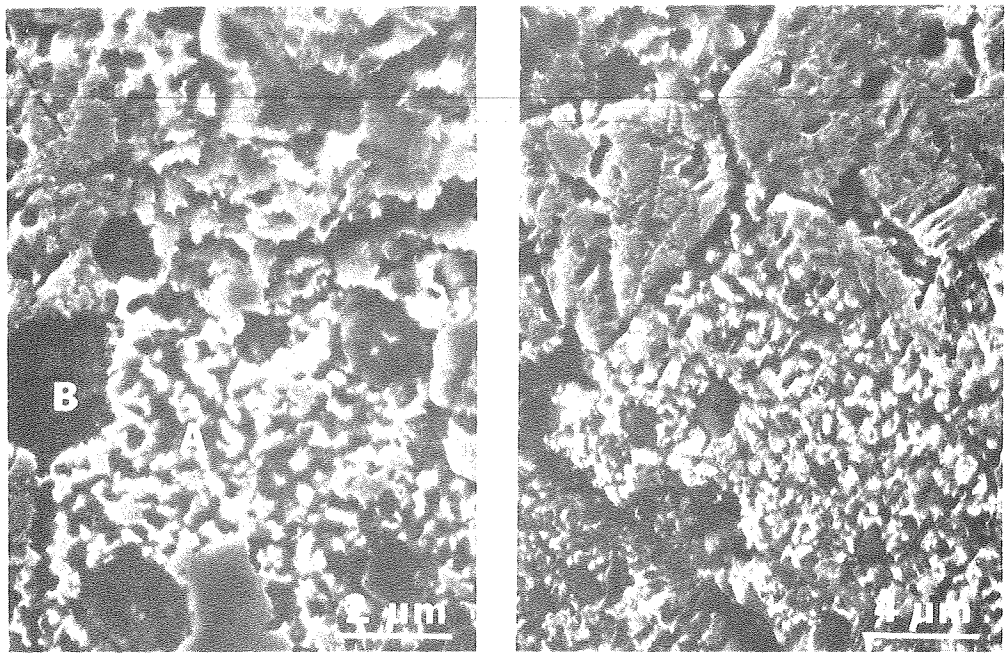

Fig. 6(a)

Figure 6b

X-RAY COMPOSITIONAL ANALYSIS

PHASE A PHASE B

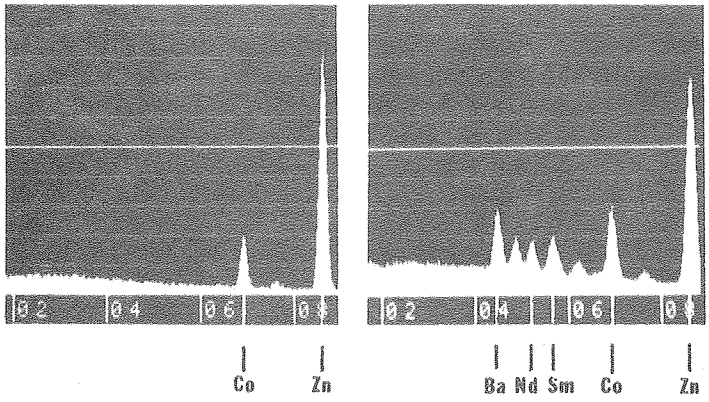

Fig. 6(b)

XBB 791-551

Figure 7a
STEM MICROGRAPH OF TWO PHASE REGION

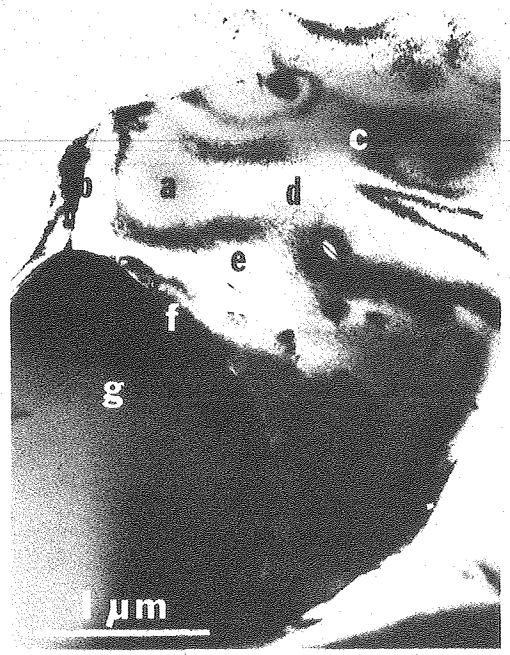

Fig. 7(a)

Figure 7b COMPOSITION GRADIENTS

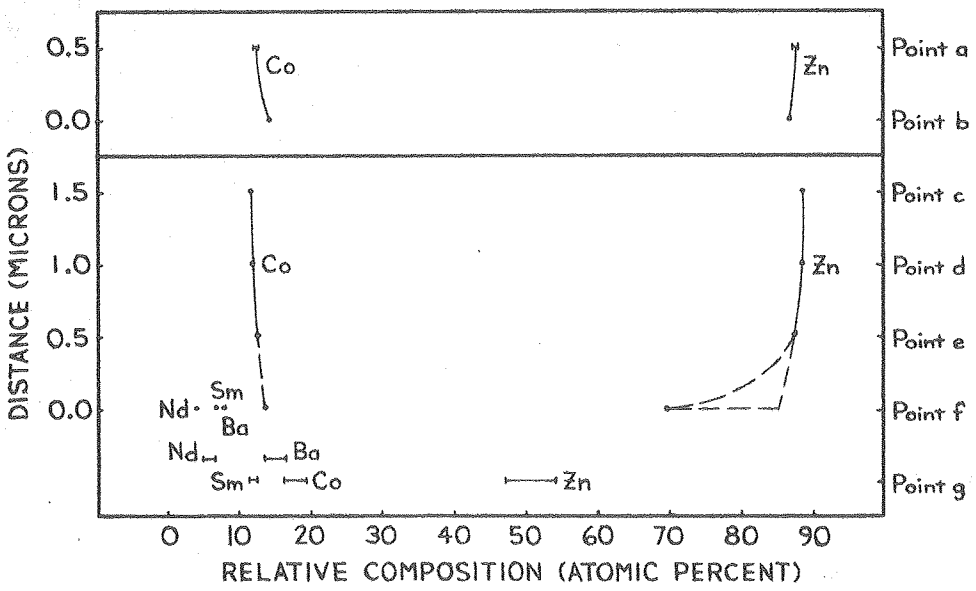

XBB 791-547

Fig. 7(b)

Figure 8a

ELECTRON DIFFRACTION PATTERNS

ZINC-COBALT OXIDE PHASE

ZINC-OTHER METALS OXIDE PHASE

INDEXED 100 PATTERN

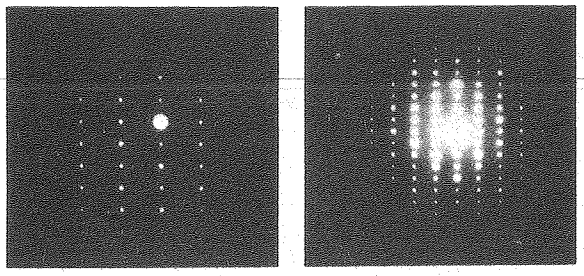

Fig. 8(a)

Figure 8b

SUGGESTED VARISTOR UNIT CELL CONFIGURATIONS

HEXAGONAL UNIT CELLS

SCALE: 1Å

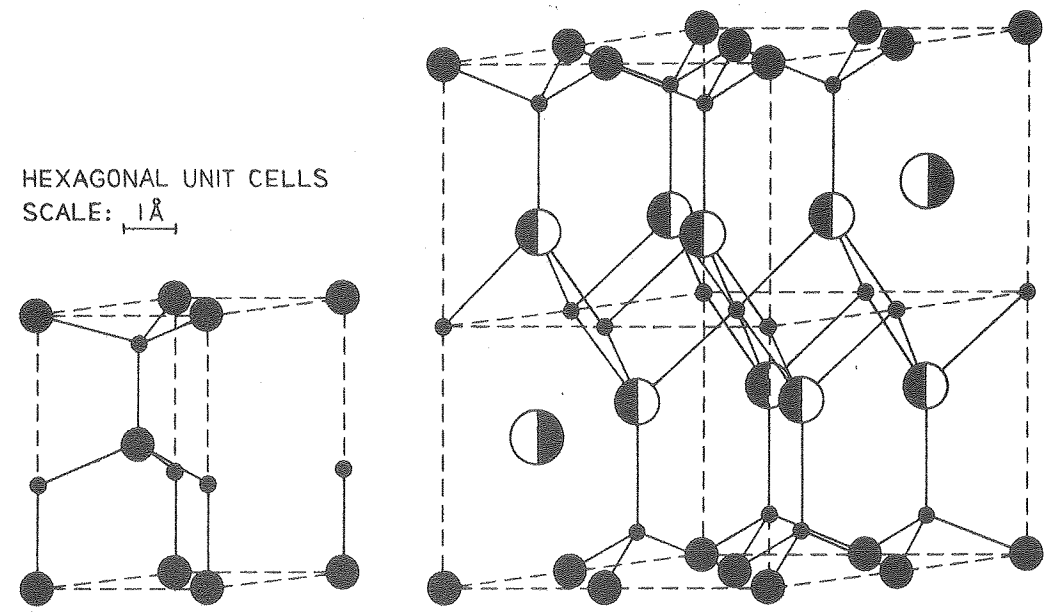

ZINC-COBALT OXIDE PHASE

- OXYGEN ION
- ZINC OR COBALT ION

ZINC-OTHER METALS OXIDE PHASE

- OXYGEN ION
- ZINC OR COBALT ION
- ZINC OR COBALT OR SAMARIUM OR NEODYMIUM ION
- BARIUM ION INTERSTITIAL

Fig. 8(b)

XBB 791-554

Figure 9

LOW MAGNIFICATION TEM MICROGRAPHS
BRIGHT FIELD-DARK FIELD PAIRS

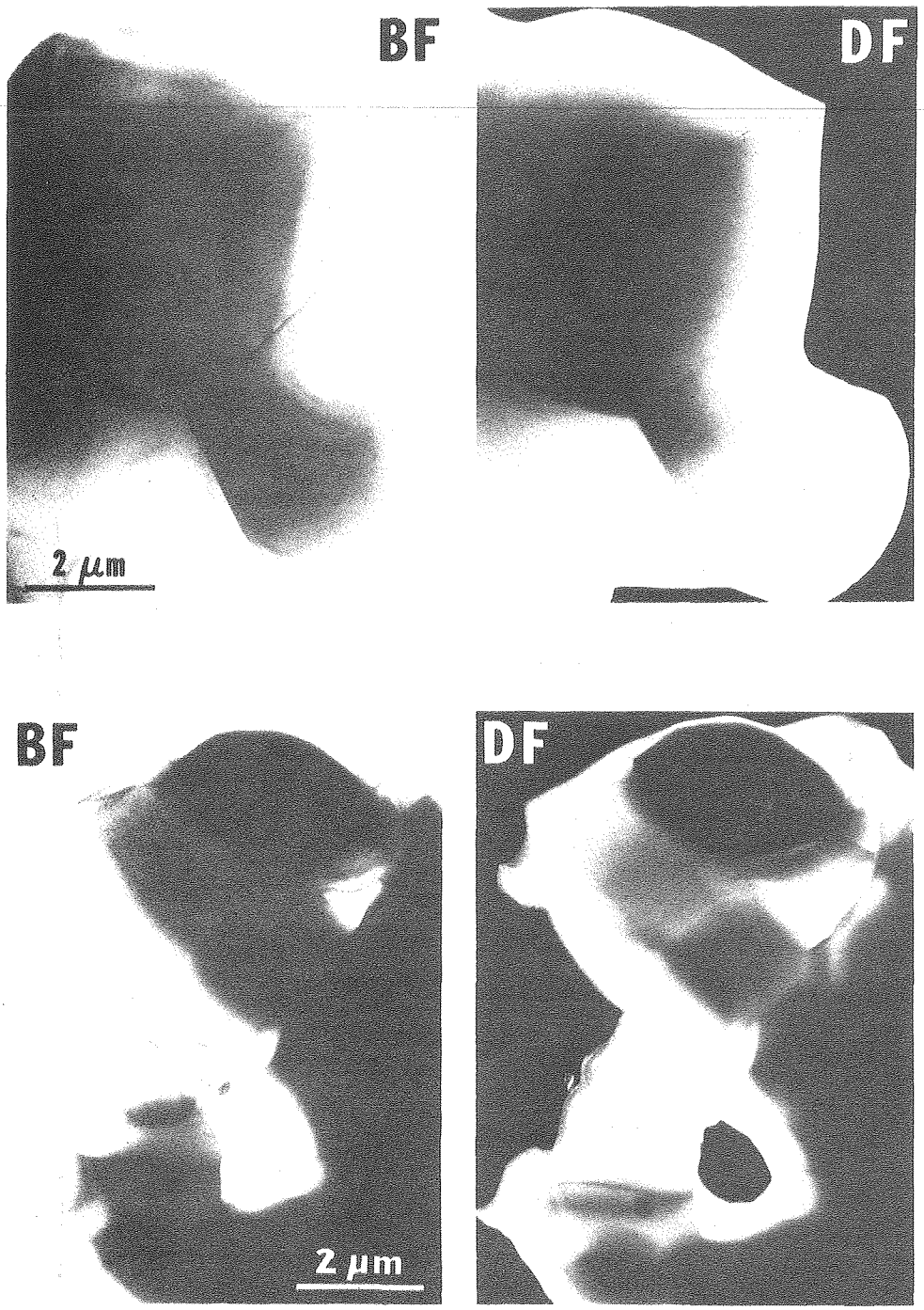

XBB 791-548

Fig. 9

Figure 10a.
TEM MICROGRAPHS
THREE-GRAIN JUNCTION

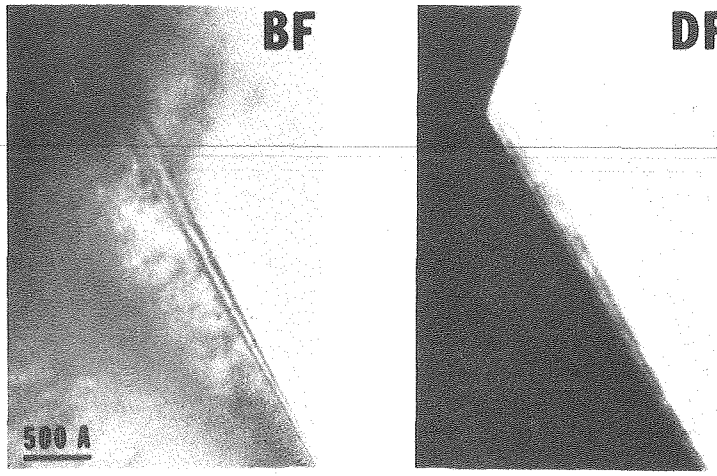

Fig. 10(a)

Figure 10b
HIGH RESOLUTION TEM MICROGRAPHS
ZINC-COBALT OXIDE GRAIN BOUNDARY

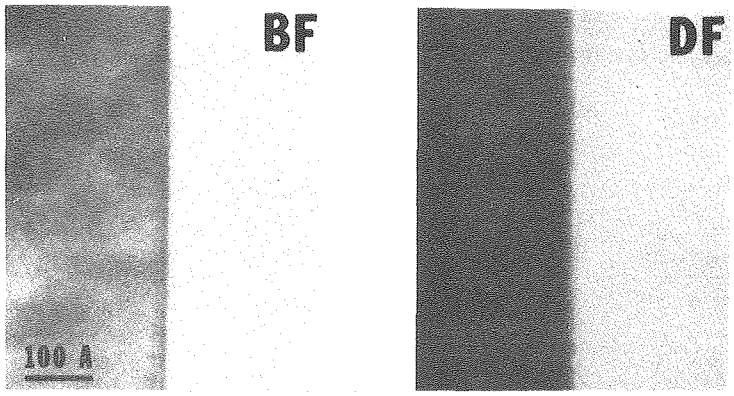

Fig. 10(b)

Figure 10c
HIGH RESOLUTION TEM MICROGRAPHS
TWO PHASE BOUNDARY

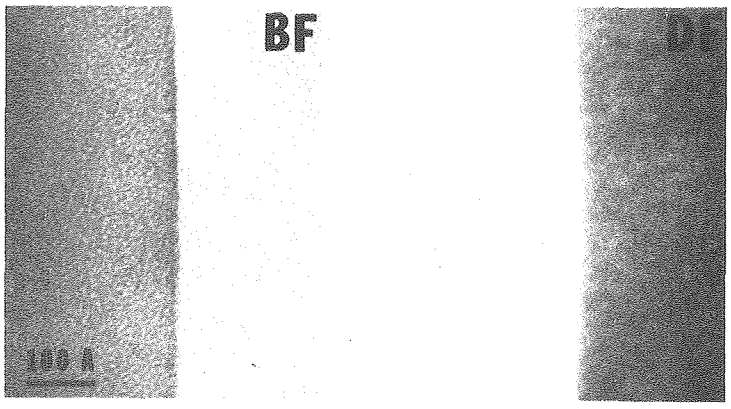

Fig. 10(c)

XBB 791-553

Figure 11

LATTICE IMAGE TEM MICROGRAPH
ZINC-COBALT OXIDE GRAIN BOUNDARY

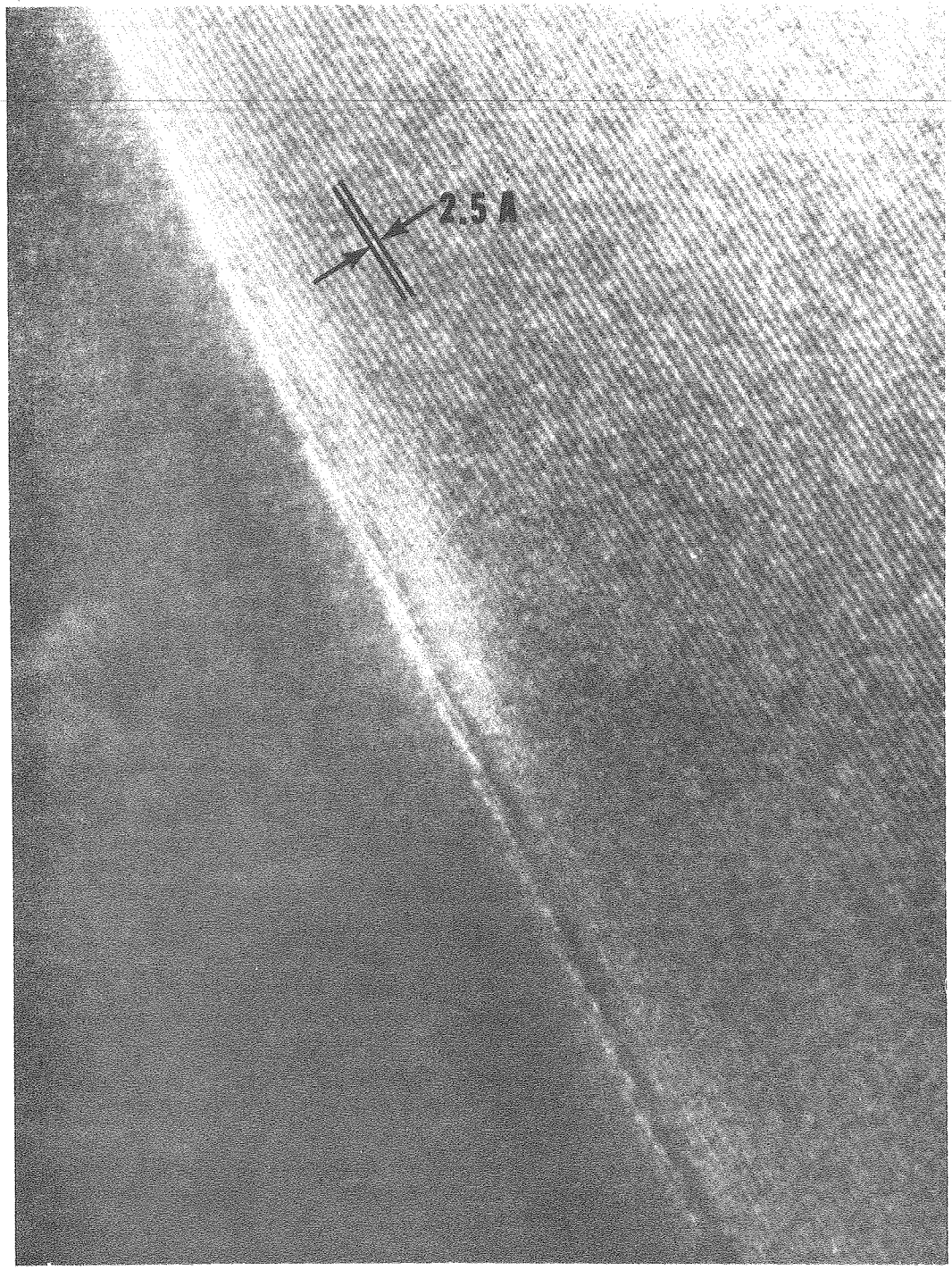

XBB 791-550

Fig. 11

FIGURE 12:
VOLTAGE CONTRAST MICROGRAPHS

NO BIAS

10-VOLT REVERSE BIAS

10-VOLT BIAS

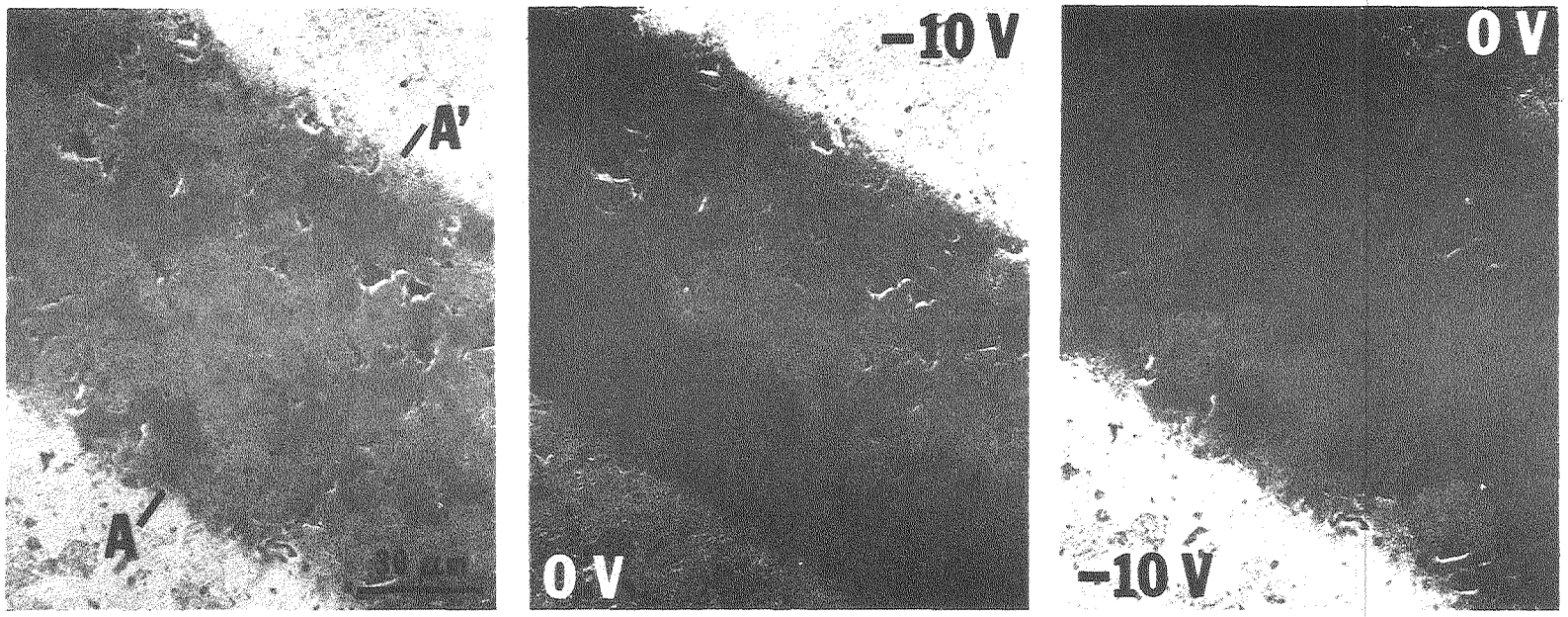

XBB 791-549

Fig. 12

FIGURE 13A:
VOLTAGE CONTRAST LINE SCANS

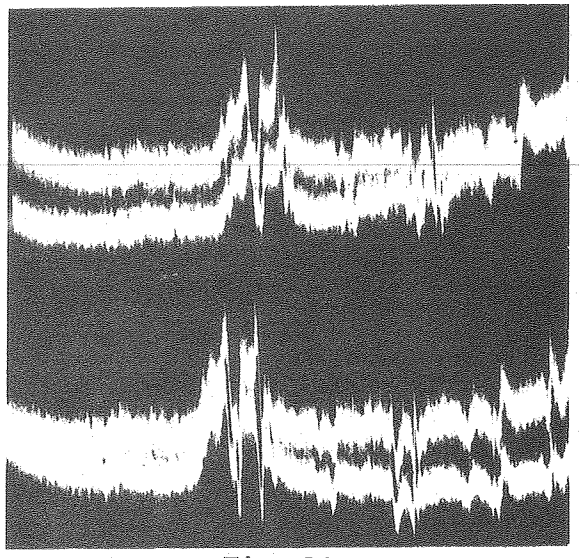

Fig. 13a

FIGURE 13B:
VOLTAGE CONTRAST LINE SCAN TRACES

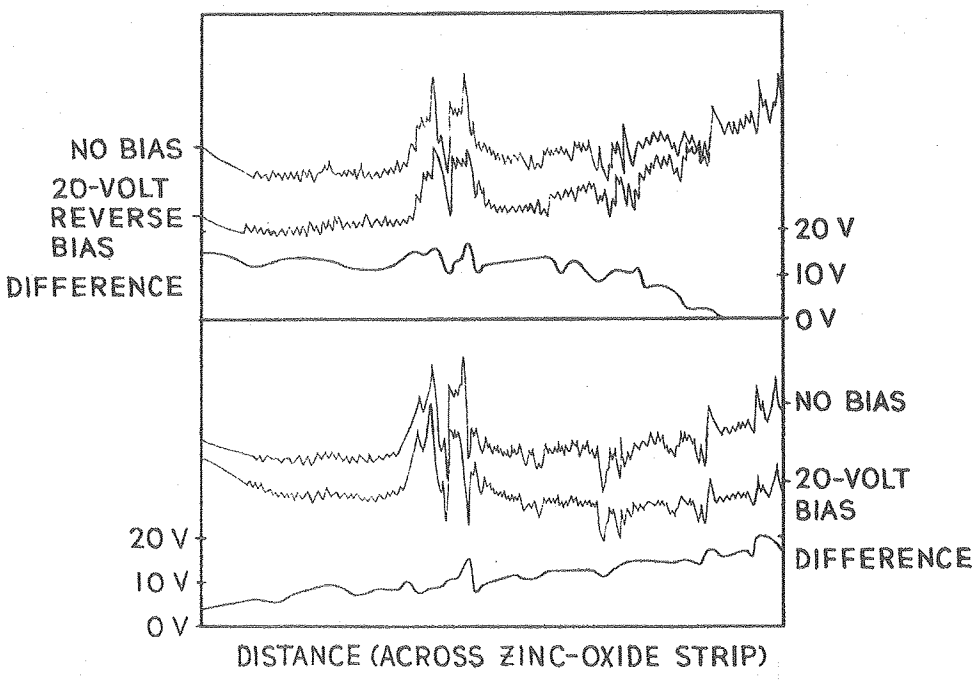

Fig. 13b

XBB 791-546

FIGURE 14A:
VOLTAGE CONTRAST MICRODENSITOMETER TRACES

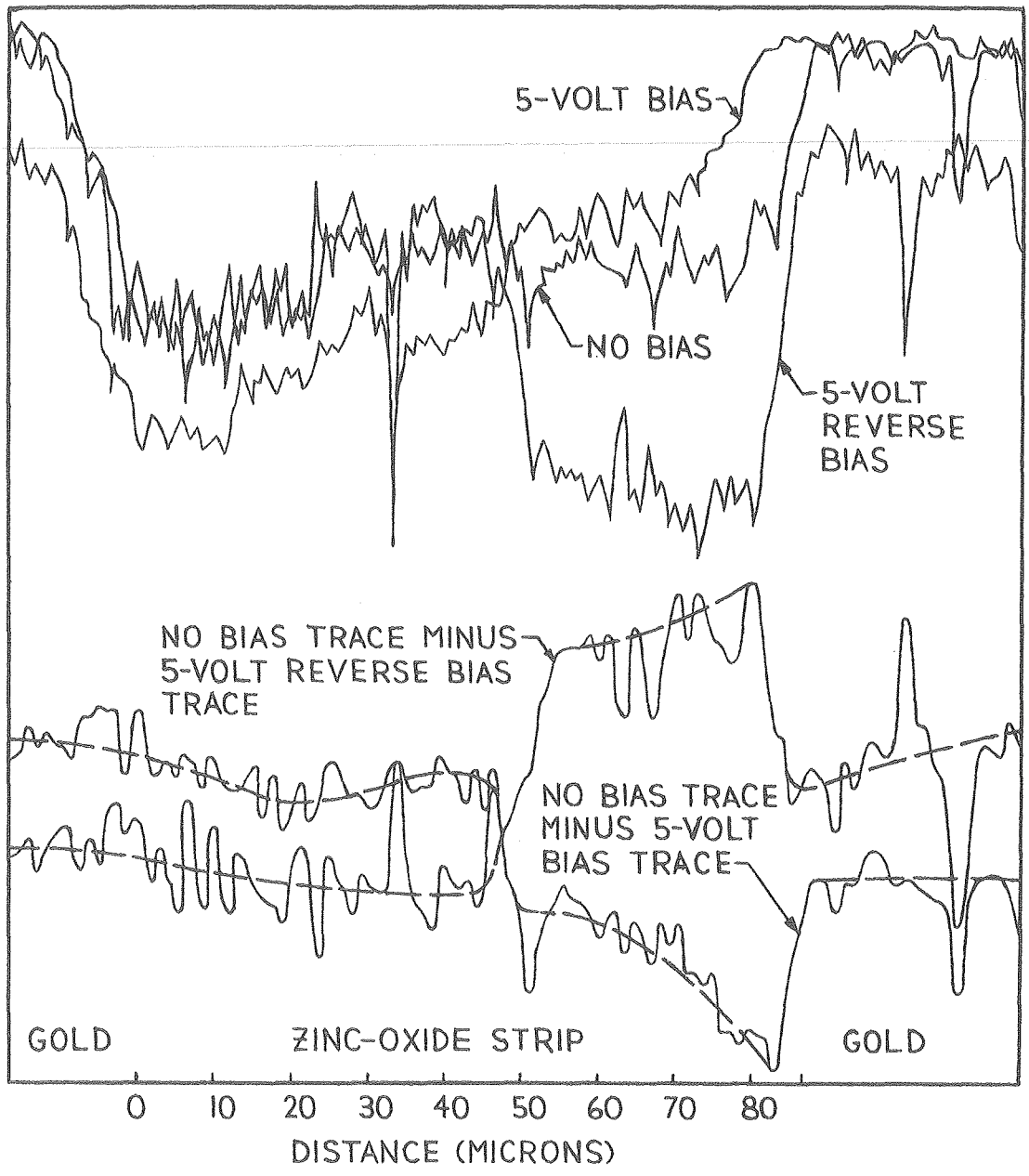

XBL 791-8032

FIGURE 14B:
VOLTAGE CONTRAST MICRODENSITOMETER TRACES

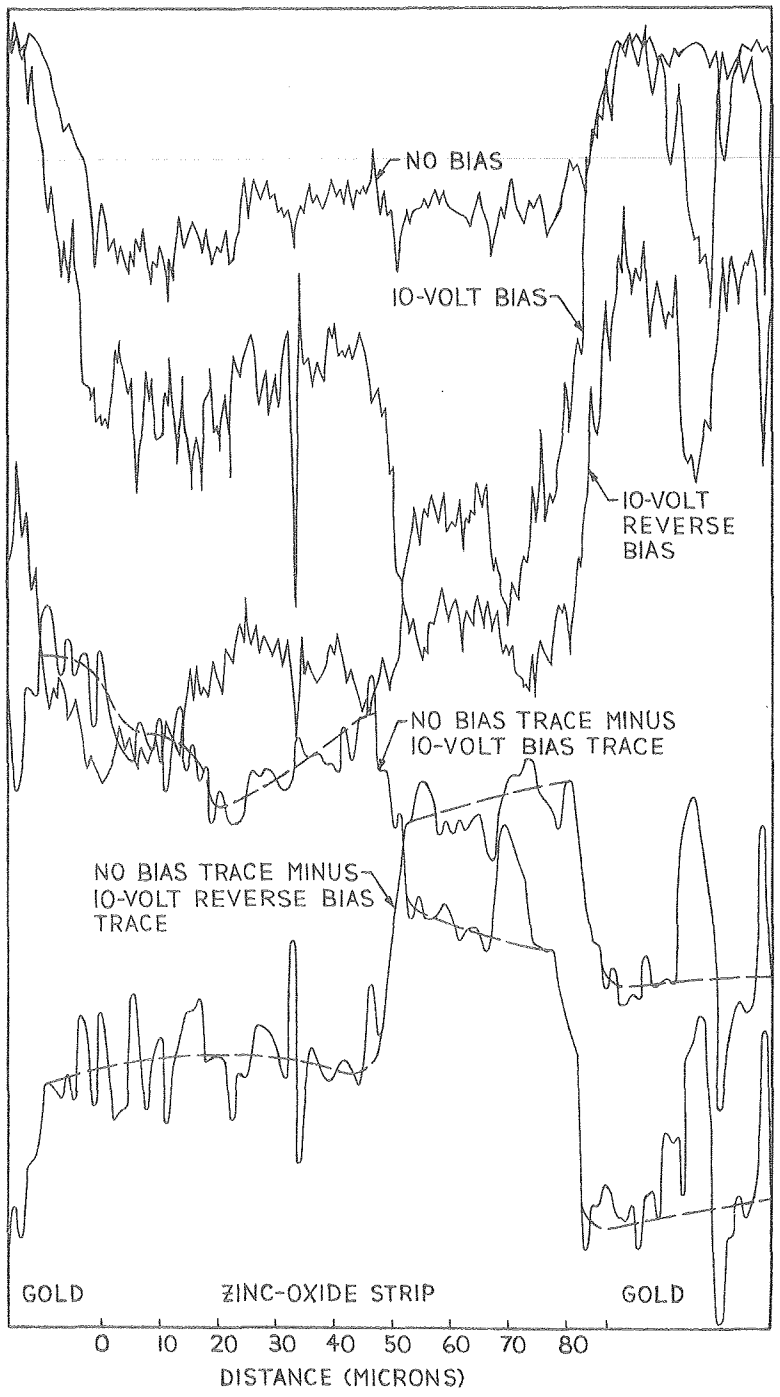

XBL 791-8029

FIGURE 14C:
VOLTAGE CONTRAST MICRODENSITOMETER TRACES

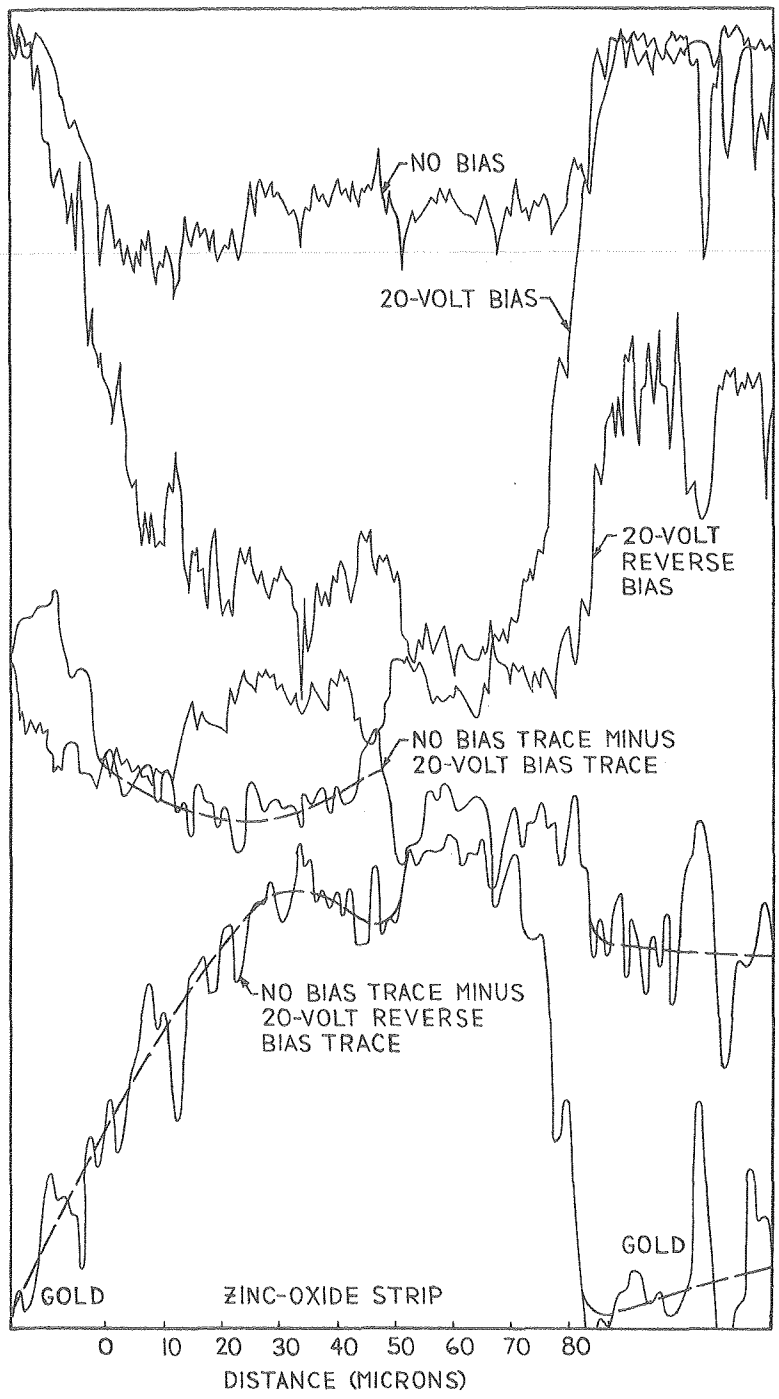

XBL 791-8030

This report was done with support from the Department of Energy. Any conclusions or opinions expressed in this report represent solely those of the author(s) and not necessarily those of The Regents of the University of California, the Lawrence Berkeley Laboratory or the Department of Energy.

Reference to a company or product name does not imply approval or recommendation of the product by the University of California or the U.S. Department of Energy to the exclusion of others that may be suitable.

TECHNICAL INFORMATION DEPARTMENT
LAWRENCE BERKELEY LABORATORY
UNIVERSITY OF CALIFORNIA
BERKELEY, CALIFORNIA 94720